Syntheses, Crystal Structures, and Fluorescence Properties of Three Coordination Polymers Constructed Based on Benzoic Acid and Its Derivatives①

LIU Guang-Zeng(刘光增);CHEN Hong-Tai(陈洪太);ZHANG Xiu-Tang②(张修堂)

(*Advanced Material Institute of Research, College of Chemistry and Chemical Engineering, Qilu Normal University, Jinan* 250013, *China*)

ABSTRACT Three new different dimensional coordination polymers, namely, $[Zn(BA^-)_2(4,4'\text{-bib})_{1.5}]_n$ (**1**), $[Zn(4\text{-BrBA}^-)_2(1,4\text{-bmb})]_n$ (**2**) and $[Mn(4\text{-BrBA}^-)_2(4,4'\text{-bib})]_n$ (**3**) have been assembled through the mixed-ligand synthetic strategy (4-HBrBA = 4-bromobenzoic acid, HBA = benzoic acid, 1,4-bmb = 1,4-bis(1H-imidazol-4-yl)benzene, 4,4′-bib = 4,4′-bis(imidazolyl)biphenyl). Their structures have been determined by single-crystal X-ray diffraction analyses and further characterized by elemental analyses (EA), powder X-ray diffraction (PXRD), and thermogravimetric (TG) analyses. Single-crystal X-ray diffraction analysis reveals that the crystals of complexes **1**～**3** are all in triclinic systems, space group $P\bar{1}$. Complexes **1** and **2** are 0D binuclear structures, and **3** is a 1D chain. Moreover, the solid state fluorescence properties of **1** and **2** have been investigated.

Keywords: 4-bromobenzoic acid;benzoic acid;1,4-bis[(1H-imidazol-1-yl)methyl]benzene;4,4′-bis(imidazolyl)biphenyl

DOI: 10.14102/j.cnki.0254-5861.2011-1626

1 INTRODUCTION

Over the past few decades, extensive experimental and theoretical efforts of coordination polymers (CPs) have attracted a great deal of interest for their regulated and interesting structural topologies as well as their potential applications in the fields of luminescence, magnetism, catalysis, gas storage, conductivity, ion exchange, nonlinear optics, and spin-transition behavior[1, 2]. Such materials are constructed from metal ions as connected centers and multifunctional organic ligands as linkers usually. In principle, the targeting assemblies with desired structural features and physicochemical properties greatly depend on the nature of organic ligands

Received 4 March 2017; accepted 18 August 2017 (**CCDC 1527398 for 1, 1527397 for 2 and 1527399 for 3**)

① Supported by the National Natural Science Foundation of China (No. 21451001) and the Key Discipline, Innovation Team, and Key Lab. of Qilu Normal University

② Corresponding author. Zhang Xiu-Tang, born in 1978, professor, majoring in inorganic chemistry. E-mail: xiutangzhang@163.com

and metal ions, among which the appropriate choice of well-designed organic building blocks is one of the most effective ways[3, 4].

Among numerous organic ligands, the carboxylic acid ligands and N-donor linkers are favored for their strong coordinating ability, which could stabilize the packing architecture. Benzoic acid and its derivatives in the structure have certain rigidity and stability. The introduction of different substituents on the aromatic ring can make the crystal structures of the complexes varied. For example, bipyridine linker as a N-donor ligand is beneficial to the syntheses of extended CPs and can generate high-dimensional structures owing to its simple bridging mode and strong coordination ability[5-7]. And the *cis*- or *trans*-configurations of bis(imidazole) linkers often cause structural diversity when they coordinate to metal centers[8-11].

Thus, these considerations inspired us to explore new coordination networks with benzoic acid and its derivatives and transition metal salts under solvothermal conditions under solvothermal conditions in the presence of bis(imidazole) linkers, respectively. Here we report the syntheses and characterizations of three CPs and a systematic comparison is made. Besides, fluorescence properties of **1** and **2** have also been investigated.

2 EXPERIMENTAL

2. 1 Generals

All chemical reagents were purchased from Jinan Henghua Sci. & Tec. Co. Ltd. without further purification. Elemental analyses were carried out on a CE instruments EA 1110 elemental analyzer. TGA was measured from 0 to 800 ºC on a SDT Q600 instrument at a heating rate of 10 ºC/min under N_2 atmosphere (100 mL/min). X-ray powder diffractions were measured on a Panalytical X-Pert pro diffractometer with Cu$K\alpha$ radiation. Fluorescence spectra were performed on a Hitachi F-4500 fluorescence spectrophotometer at room temperature.

2. 2 Syntheses

2. 2. 1 Synthesis of $[Zn(BA^-)_2(4,4'\text{-bib})_{1.5}]_n$ (1)

The mixture of HBA (0.20 mmol, 0.024 g), 4,4′-bib (0.30 mmol, 0.085 g), $Zn(OAC)_2$ (0.30 mmol, 0.066 g), 12 mL H_2O, and NaOH (0.40 mm, 0.016g) was sealed in a 25 mL Teflon-lined stainless-steel vessel and heated to 170 ℃ for 3 days, and followed by slow cooling to room temperature at a descent rate of 10 ºC/h. Yield of 47% (based on HBA). Anal. Calcd. (%) for $C_{82}H_{62}N_{12}O_8Zn_2$: C, 66.81; H, 4.21; N, 11.40. Found (%): C, 65.62; H, 4.72; N, 11.30.

2. 2. 2 Synthesis of $[Zn(4\text{-}BrBA^-)_2(1,4\text{-bmb})]_n$ (2)

The mixture of 4-HBrBA (0.20 mm, 0.040 g), 1,4-bmb (0.20 mm, 0.047 g), $ZnSO_4$ (0.40 mm, 0.115 g), 12 mL H_2O and NaOH (0.30 mm, 0.012 g) was sealed in a 25 mL Teflon-lined stainless-steel vessel and heated to 170 ℃ for 3 days, and followed by slow cooling to room temperature at a rate of 10 ºC/h. Coreless block crystals of **2** were obtained. Yield of 39% (based on HBrBA). Anal. Calcd. (%) for $C_{56}H_{44}Br_4N_8O_8Zn_2$: C, 47.79; H, 3.12; N, 8.67. Found (%): C, 48.23; H, 3.54; N, 8.92.

2. 2. 3 Synthesis of $[Mn(4\text{-}BrBA^-)_2(4,4'\text{-}bib)]_n$ (3)

The synthetic method is similar to that of complex **2** except that 1,4-bmb and $ZnSO_4$ were replaced by 4,4′-bib and $MnSO_4$. Colorless block crystals of **3** were obtainedin 33% yield (based on HBrBA). Anal. Calcd. (%) for $C_{34}H_{22}Br_2MnN_2O_4$: C, 55.34; H, 2.98; N, 3.80. Found (%): C, 54.28; H, 3.09; N, 3.96.

2. 3 Structure determination

Structural integrity single crystals of **1**～**3** were carefully selected under an optical microscope and fixed to thin glass fibers. After that, single-crystal X-ray diffraction analyses were performed on a Siemens SMART diffractometer using Mo-$K\alpha$ radiation (λ = 0.71073Å) at 296(2) K. The absorption correction was based on multiple and symmetry-equivalent reflections in the data set using the SADABS program based on the method of Blessing. The structure was solved by direct methods and refined by full-matrix least-squares techniques using the SHELXS-97 package, and further refined by SHELXL-97 procedure. All non-hydrogen atoms were refined anisotropically[12]. All the hydrogen atoms except those for water molecules were generated geometrically with fixed isotropic thermal parameters, and included in the structure factor calculations. The hydrogen atoms attached to oxygen were refined with O–H = 0.85 Å and U_{iso}(H) = 1.2U_{eq}(O). The crystallographic data and details for complexes **1**～**3** are listed in Table 1., and their elected bond lengths and bond angles are shown in Table 2.

3 RESULTS AND DISCUSSION

3. 1 Structure description of $[Zn(BA^-)_2(4,4'\text{-}bib)_{1.5}]_n$ (1)

X-ray crystallography reveals that **1** is a zero-dimensional structure and crystallizes in the triclinic system, space group $P\bar{1}$. As shown in Fig. 1, the asymmetric unit consists of one Zn^{II} ion, two completely deprotonated BA^- ligands, and one and a half 4,4′-bib ligands. Zn^{II} is located in a distorted $\{ZnN_2O_3\}$ hexahedral geometry, completed by two carboxyl groups from two distinct BA^- ligands and two N atoms from two 4,4′-bib ligands, with τ_5 = 0.441 ($\tau_5 = |\beta - \alpha|/60°$, in which α and β are the two largest bond angles in the five-coordinate complex: α = ∠N(5)Zn(1)O(2) = 118.87°, β = ∠O(1)Zn(1)O(3) = 145.34°)[13]. The Zn−O bond lengths fall in the normal range of 1.9310(19)～2.8128(26) Å, and the Zn–N bond lengths are 2.0003(26) and 2.0167(28) Å, respectively.

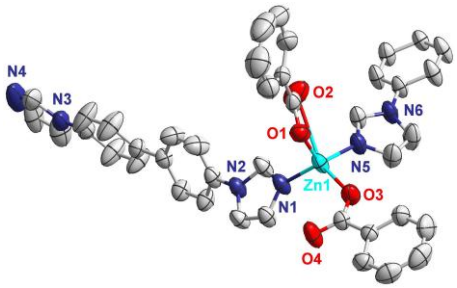

Fig. 1. Coordination environment of Zn^{II} ion in complex 1

Two Zn^{II} ions are linked by one 4,4′-bib to form a 0D binuclear structure. Each Zn^{II} ion coordinates with two BA^- ligands which adopted μ^1-η^1 and μ^1-η^2 coordination modes respectively, and two single-connected 4,4′-bib ligands. Structure of the complex exhibits a centrosymmetric character. Zn···Zn distances are 17.9276(10) Å, as shown in Fig. 2a.

Adjacent molecules are linked through C–H···O and C–H···N hydrogen bonding interactions (H···A are between 2.35 and 2.57 Å) to form a 3D supramolecular structure (Fig. 2b). The hydrogen bonding data for complex **1** are summarized in Table 3.

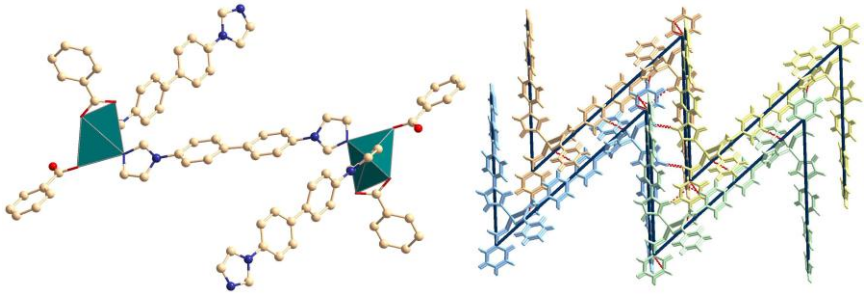

(a) **(b)**

Fig. 2. (a) Binuclear structure of 1 viewed along the *c* axis. (b) 3D supramolecular structure of complex 1

3. 2 Structure description of $[Zn(4\text{-}BrBA^-)_2(1,4\text{-}bmb)]_n$ (2)

X-ray crystallography reveals that **2** is a zero-dimensional structure and crystallizes in triclinic system, space group $P\bar{1}$. As shown in Fig. 4, the asymmetric unit consists of one Zn^{II} ion, two 4-$BrBA^-$ ligands, and one 1,4-bmb ligand (Fig.3). The Zn^{II} ion is located in a slightly distorted $\{ZnN_2O_3\}$ hexahedral coordination environment, completed by two carboxyl groups from two distinct 4-$BrBA^-$ ligands, and two N atoms from two 1,4-bmb ligands, with $\tau_5 = 0.856$ ($\tau_5 = |\beta - \alpha|/60$ °, in which α and β are the two largest bond angles in the five-coordinate complex: $\alpha = \angle O(1)Zn(1)O(3) = 165.88$ °, $\beta = \angle N(1)Zn(1)N(3) = 114.54$ °). The Zn−O bond lengths vary from 1.9352(37) to 2.7170(33) Å, and the Zn−N bond distances are in the normal range of 1.9994(35)～2.0220(48) Å.

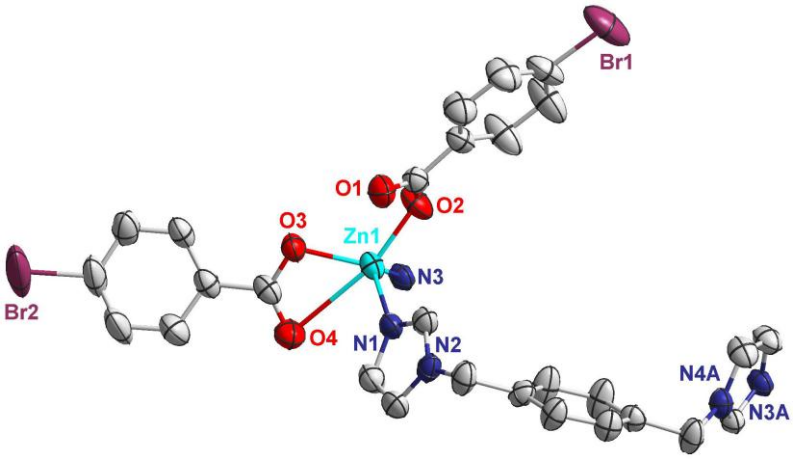

Fig. 3. Asymmetric unit of complex 2 (Symmetry code: A: 2–*x*, 2–*y*, 1–*z*)

HBrBA is completely deprotonated and exhibits μ^1-η^1 and μ^2-η^1:η^1 coordination modes, respectively. Two Zn^{II} ions are linked by two flexible 1,4-bmb ligands to form a binuclear structure, with the dihedral angles between the central phenyl ring and two imidazole rings to be 88.02 and 75.54°, respectively. Structure of the complex exhibits a centrosymmetric character, with the Zn···Zn distance being 10.79(7) Å.

Adjacent molecules are further joined by hydrogen bonds to form 3D supramolecular structures (Fig. 4a), and the lengths of hydrogen bonds (H···A) are between 2.43 and 2.61 Å. Complexes **1** and **2** have similar hydrogen bonding connections. The hydrogen bonding data for **2** are summarized in Table 3. We plotted the partial $\pi\cdots\pi$ packing interaction. The center distance of two parallel imidazole ring planes is 3.979 Å, and the lateral displacement distance between the two centers is 1.938 Å (Fig. 4b).

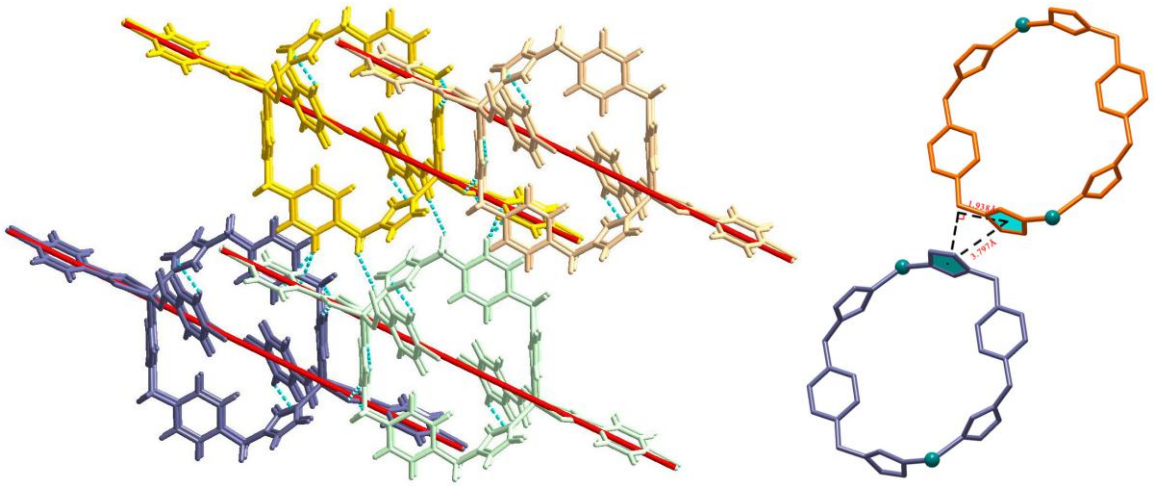

(a) **(b)**

Fig. 4. (a) 3D supramolecular structure of complex 2. (b) π-π stacking interaction in complex 2

3. 3 Structure description of $[Mn(4\text{-}BrBA^-)_2(4,4'\text{-bib})]_n$ (3)

X-ray crystallography reveals that **3** is a one-dimensional structure and crystallize in the triclinic system, space group $P\bar{1}$. As shown in Fig. 7, the asymmetric unit consists of one Mn^{II} ion, two 4-$BrBA^-$ ligands, and one 4,4′-bib ligand (Fig. 5). The Mn^{II} ion is located in a distorted $\{MnN_2O_4\}$ octahedral coordination environment completed by three carboxyl groups from three 4-$BrBA^-$ ligands which adopted μ^1-η^2 and μ^2-η^1:η^1 coordination modes respectively, and two N atoms from two different 4,4′-bib ligands. The Mn–O/N bond lengths fall in the normal 2.1091(22)～2.2533(35) Å region.

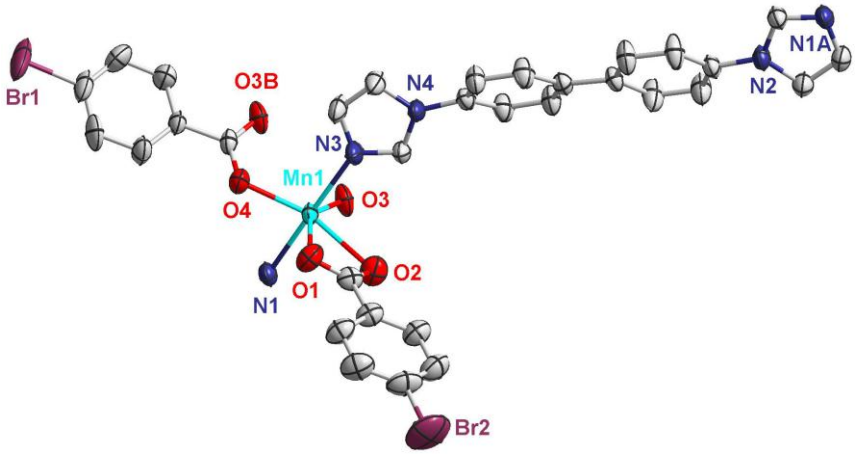

Fig. 5. Asymmetric unit of 3 (Symmetry codes: A: 1+*x*, *y*, 1+*z*; B: 1–*x*, 2–*y*, 1–*z*)

Each 4,4′-bib ligand connects with two Mn^{II} ions and further extends into two abreast chains, with the dihedral angles between two phenyl rings being 0 °or 7.35 °, and 0 °or 5.14 °for two terminal imidazole rings. The 4-$BrBA^-$ ligand (μ^2-η^1:η^1) bridged two adjacent Mn^{II} ions to make the two abreast chains form a binuclear chain, with the distance between two adjacent Mn^{II} ions to be 4.099 Å (Fig. 6a). Owing to the presence of C–H···Br and C–H···O hydrogen bonds, complex **3** links from 1D binuclear chain into a 3D supramolecular structure (Fig. 6b). The hydrogen bonding data for complex **3** are illustrated in Table 3.

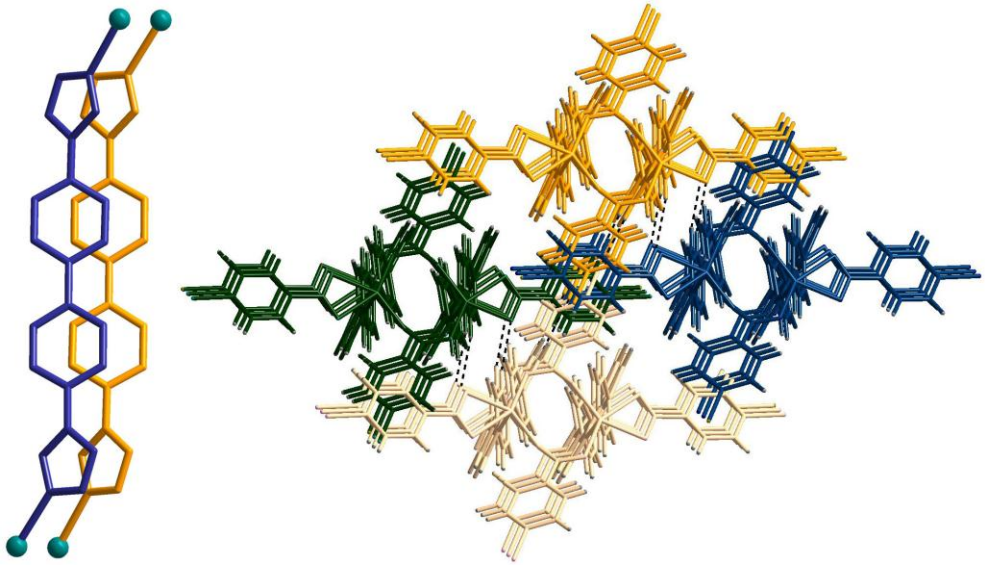

(a) **(b)**

Fig. 6. (a) Chain of {Mn(μ^2-4,4′-bib)}$_n$ in complex 3. (b) 3D supramolecular structure of complex 3

Three different dimensions CPs have been constructed from the mixed ligand of benzoic acid and its derivatives and two bis(imidazole) linkers (4,4′-bib, 1,4-bmb). The sundry coordination modes of the carboxyl groups and the deformation ability difference of the ancillary ligands lead to the formation of complexes with different structures in different dimensions. The three structures reveal that benzoic acid and its derivatives are effective ligands with rich coordination modes, which is useful to better understand the synthon selectivity in multifunctional crystal structures.

3. 4 Powder X-ray diffraction

In order to check the phase purity of these complexes, the PXRD patterns of the title complexes were checked at room temperature. As shown in Fig. 7, the peak positions of the simulated and experimental PXRD patterns are in agreement with each other, demonstrating good phase purity of the complexes. The dissimilarities in intensity may be due to the preferred orientation of the crystalline powder samples.

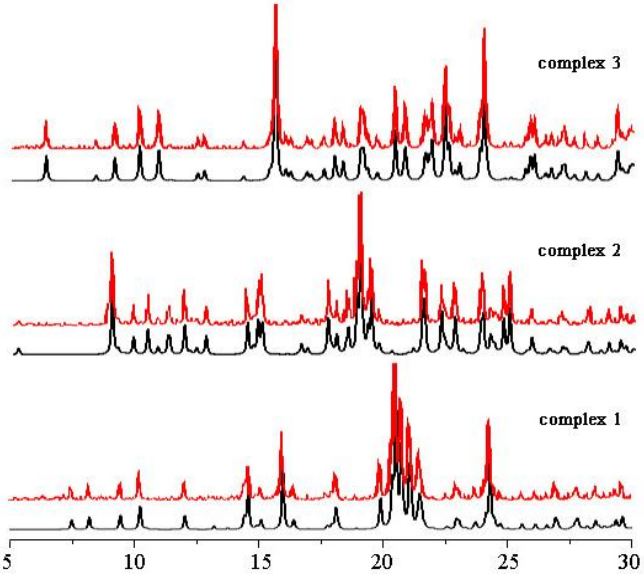

Fig. 7. PXRD patterns of complexes 1～3. Black: calculated from the X-ray single-crystal data; Red: observed for the as-synthesized solids

3. 5 Thermogravimetric analysis

To study the stability of these polymers, thermogravimetric analyses (TGA) of complexes **1**～**3** were performed (Fig. 8). The TGA curve of these complexes indicates that the framework of complex **1** begins to collapse from 285 ℃, while complexes **2** and **3** are more stable up to 330 ℃, where the decomposition of the framework starts. The resulting residue of compounds **1** and **2** remains as ZnO (calcd.: 9.1%, found: 11.8% for **1**; calcd.: 11.3%, found: 13.6% for **2**) after the complete decomposition of organic ligands. In compound **3**, at about 710 ℃, it decomposes completely and the remaining residue is presumed to be Mn_2O_3 (calcd.: 11.1%; found: 13.3%).

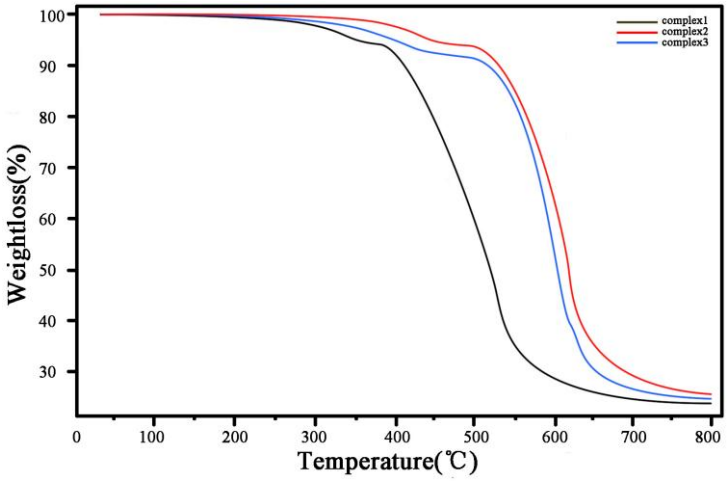

Fig. 8. TGA curves for complexes 1～3

3. 6 Photoluminescent investigation

The emission spectra of complexes **1** and **2** and free ligands in their solid states are investigated at room temperature under the same conditions. As depicted in Fig. 9, the emission spectra of 4,4′-bib and complex **1** show the main peaks at 359 nm (λ_{ex} = 307 nm) and 373 nm (λ_{ex} = 332 nm), respectively. Moreover, the 1,4-bmb and complex **2** show the main peaks at 524 nm (λ_{ex} = 489 nm) and 509 nm (λ_{ex} = 496 nm), respectively. By comparing the two groups, both ligands and complexes have similar emission peaks. The difference between them is reflected in the variation of relative intensity of the two emission peaks, which can be assigned to the intraligand ($\pi^*\rightarrow$n or $\pi^*\rightarrow\pi$) emission because these emissions are neither metal-to-ligand charge transfer (MLCT) nor ligand-to-metal transfer (LMCT) in nature since the Zn^{II} ions are difficult to oxidize or reduce due to its d^{10} configuration [14]. The difference of the emission behaviors for complexes **1** and **2** probably derives from the different conformations of organic ligands as well as the differences in the rigidity of solid state crystal packing structures. Because of the good photoluminescence properties, complexes **1** and **2** can be used as potential photosensitive materials.

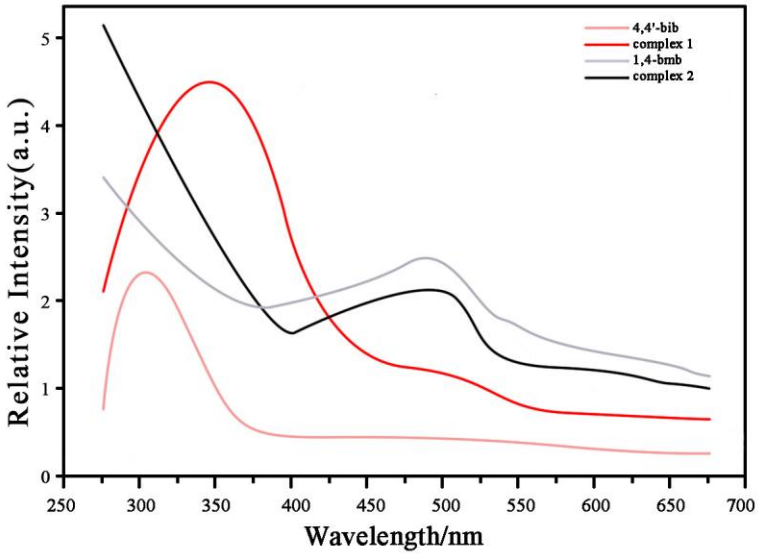

Fig. 9. Emission spectra of free ligands and complexes 1 and 2 in the solid state at room temperature

REFERENCES

(1) (a) Baldo, M. A.; Lamansky, S.; Burrows, P. E.; Thompson, M. E.; Forrest, S. R. Very high-efficiency green organic light-emitting devices based on electro-phosphorescence. *Applied. Physics. Letters* **1999**, 75, 4–6. (b) Zhao, E. X. ; Li, F. F.; Zhao, D. Hydrothermal syntheses, crystal structures and characteristics of two new isostructural Ni(II) coordination polymers. *Chin. J. Struct. Chem*. **201**6, 35, 1764–1769.

(2) (a) Zhao, W.; Shen Z. H.; Xing, J. H.; Xu, T. M.; Peng, W. L.; Liu, X. H. Synthesis, characterization, nematocidal activity and docking study of novel pyrazole-4-carboxamide derivatives. *Chin. J. Struct. Chem.* **2017**, 36, 423–428. (b) Chen, S. S. The roles of imidazole ligands in coordination supramolecular systems. *CrystEngComm*. **2016**, 18, 6543–6565.

(3) (a) Hao, X. N.; Zheng, B. H.; Hu, T. P. Syntheses and characterizations of Cd(II) and Pr(III) complexes based on 5-(tetrazol-5-yl) isophthalic acid. *Chin. J. Struct. Chem*. **2016**, 35, 1186–1194. (b) O´Donovan, M. E.; LaDuca, R. L. Zinc coordination polymers containing substituted isophthalate ligands and fragments from in situ hydrolysis of 4-pyridylisonicotinamide. *J. Mol. Struct*. **2015**, 1083, 212–220.

(4) (a) Fan, L. M.; Zhang, X. T.; Li, D. C.; Sun, D.; Zhang, W.; Dou, J. M. Supramolecular isomeric flat and wavy honeycomb networks: additive agent effect on the ligand linkages. *CrystEngComm.* **2013**, 15, 349–355. (b) Zhang, X. T.; Fan, L. M.; Sun, Z.; Zhang, W.; Fan, W. L.; Sun, L. M.; Zhao, X. Syntheses, structures, and luminescence of four lanthanide metal-organic frameworks based on lanthanide-oxide chains with *C2*- or *C3*-symmetric trigonal-planar polycarboxylate ligands. *CrystEngComm.* **2013**, 15, 4910–4916.

(5) (a) Gao, Y.; Fan, L. M.; Song, W. K.; Liu, X. Z.; Zhang, X. T. Synthesis, crystal structure, and topology analysis of one novel interpenetrated 2D cobalt coordination polymer, {[Co(HBTB)(4,4′-btb)] H_2O}$_n$. *Chin. J. Struct. Chem.* **2014**, 33, 1333–1338. (b) Zhang, X. T.; Fan, L. M.; Zhang, W.; Ding, Y. S.; Zhao, X. One highly photocatalytic polyoxomolybdate compound constructed from novel-type triple helix {Mo_4O_{12}}$_n$ chains and copper(I)-organic nets. *Dalton Trans.* **2013**, DOI: 10.1039/c3dt52001c.

(6) Han, L.; Qin, L.; Yan, X. Z.; Xu, L. P.; Sun, J. L.; Yu, L.; Chen, H. B.; Zou, X. D. Two isomeric magnesium metal-organic frameworks with [24-MC-6] metallacrown cluster. *Cryst. Growth Des.* **2013**, 13, 1807–1811.

(7) Gong, Y. Q.; Mi, T. Q.; Liang, W. T. Synthesis, crystal structure and properties of a 3-fold interpenetrating 3D Cd(II) complex derived from 4-(2-methyl-1H-imidazol-1-yl)benzoic acid. *Chin. J. Struct. Chem.* **2016**, 35, 1600–1605.

(8) Chen, P. K.; Li, Q. C.; Grindy, S.; Andersen, N. H. White-light-emitting lanthanide metallogels with tunable luminescence and reversible stimuli-responsive properties. *J. Am. Chem. Soc.* **2015**, 137, 11590–11593.

(9) Liu, Q. X.; Yao, Z. Q.; Zhao, X. J.; Zhao, Z. X.; Wang, X. G. NHC metal (silver, mercury, and nickel) complexes based on quinoxaline-dibenzimidazolium salts: synthesis, structural studies and fluorescent chemosensors for Cu^{2+} by charge transfer. *Organometallics* **2013**, 32, 3493−3501. (b) Yang, Y. M.; Zhao, Q.; Feng, W.; Li, F. Y. Luminescent chemodosimeters for bioimaging. *Chem. Rev.* **2013**, 113, 192−270.

(10) (a) Jassal, A. K.; Sharma, S.; Hundal, G.; Hundal, M. S. Structural diversity, thermal studies, and luminescent properties of metal complexes of dinitrobenzoates: a single crystal to single crystal transformation from dimeric to polymeric complex of copper(II). *Cryst. Growth. Des.* **2015**, 15, 79−93. (b) Mei, Y. X.; Xu, F.; Wei, Z. H.; Cai, H. pH dependent supramolecules based on co-crystallization of pyrazine-2,3,5,6-tetracarboxylic acid with 4,4′-bipyridine through intermolecular hydrogen bonds. *Chin. J. Struct. Chem.* **2016**, 35, 1031–1037.

(11) Zhang, X. T.; Fan, L. M.; Sun, Z.; Zhang, W.; Li, D. C.; Dou, J. M.; Han, L. Syntheses, structures, and properties of a series of multidimensional metal-organic polymers based on 3,3′,5,5′-Biphenyltetracarboxylic acid and N-donor ancillary ligands. *Cryst. Growth Des.* **2013**, 13, 792–803.

(12) (a) The network topology was evaluated by the program “TOPOS-4.0”, see: *http://www.topos.ssu.samara.ru*.
(b) Sheldrick, G.M. *SHELXTL NT Version 5.1. Program for Solution and Refinement of Crystal Structures*. University of Gőtingen, Germany **1997**.

(13) (a) Yang, L.; Powell, D. R.; Houser, R. P. Two 2D cobalt(II) coordination frameworks with unusual binodal network topology: synthesis, structures, and catalytic properties. *Dalton Trans.* **2007**, 955–964. (b) Takashima, I.; Kawagoe, R.; Hamachi, I.; Ojida, A. Development of a logic-gate-type fluorescent probe for ratiometric imaging of autolysosome in cell autophagy. *Chem. Eur. J.* **2015**, 21, 2038–2044.

(14) (a) Kong, Z. G.; Guo, S. N.; Yu, M.; Feng, S. Y.; Hu, B. A new luminescent Cd(II) coordination polymer constructed by mixed 1,4-naphthalenedi-carboxylate and N-donor chelating ligand. *Chin. J. Struct. Chem.* **2016**, 35, 591–596. (b) Guo, F. Hydrothermal syntheses, crystal structure and luminescent properties of four zinc(II) coordination polymers based on tipodal imidazole. *Inorg. Chim. Acta.* **2013**, 399, 79–84. (b) Zhan, P. Y.; Jian, J. Y.; Niu, Y. L.; Wang, Z. T.; Li, X. M. Synthesis, crystal structure and fluorescent property of a 2D network Zn(II) coordination polymer based on oxalic acid and bis(imidazol) ligand. *Chin. J. Inorg. Chem.* **2013**, 29, 424–428.

Table 1. Crystallographic Data and Details of Diffraction Experiments for Complexes 1, 2 and 3

Complex	**1**	**2**	**3**
Empirical formula	$C_{82}H_{62}N_{12}O_8Zn_2$	$C_{56}H_{44}Br_4N_8O_8Zn_2$	$C_{34}H_{22}Br_2MnN_2O_4$
Formula weight	1474.18	1407.37	737.30
Crystal system	Triclinic	Triclinic	Triclinic
Space group	$P\bar{1}$	$P\bar{1}$	$P\bar{1}$
a (Å)	10.1088	10.064	10.300
b (Å)	10.4322	12.754	11.250
c (Å)	17.4398	13.162	13.963
α (°)	98.9240	63.84	85.09
β (°)	96.3030	80.86	86.01
γ (°)	105.7140	68.59	70.34
V (Å^3)	1726.55	1411.7	1516.6
Z	1	1	2
D_c (g cm^{-3})	1.418	1.655	1.615
F(000)	762	700	734
μ(Mo*K*α) / mm^{-1}	0.764	3.741	3.111
Reflections collected	9021	7385	7912
θ range for data collection (°)	1.20～25.00	1.72～25.00	1.93～25.00
Refinement method	Full-matrix least-squares on F^2		

Data / restraints / parameters	6060/0/469	4955 / 0 / 352	5315 / 0 / 388
Goodness-of-fit on F^2	1.003	1.000	1.004
R, wR ($I > 2\sigma(I)$)	0.0411, 0.0943	0.0573, 0.1533	0.0608, 0.1803
R, wR (all data)	0.0607, 0.1079	0.0951, 0.1720	0.0846, 0.1966
Largest diff. peak and hole (e·Å^{-3})	0.330 and –0.285	1.261 and –1.478	1.546 and –1.439

Table 2. Selected Bond Lengths (Å) and Bond Angles (°) for 1～3

Complex **1**			
N(1)–Zn(1)	2.001(2)	N(5)–Zn(1)	2.017(2)
O(2)–Zn(1)	1.934(2)	O(3)–Zn(1)	1.931(2)
C(1)–N(1)–Zn(1)	124.4(2)	C(2)–N(1)–Zn(1)	129.2(2)
C(33)–N(5)–Zn(1)	131.3(2)	C(34)–N(5)–Zn(1)	122.9(2)
C(26)–O(2)–Zn(1)	112.9(2)	C(19)–O(3)–Zn(1)	127.34(19)
O(3)–Zn(1)–N(1)	118.04(10)	O(2)–Zn(1)–N(1)	109.41(10)
O(3)–Zn(1)–N(5)	95.59(9)	O(2)–Zn(1)–N(5)	118.88(10)
N(1)–Zn(1)–N(5)	110.32(10)		
Symmetry transformations used to generate the equivalent atoms: #1: –x+3, –y+1, –z+1			
Complex 2			
Zn(1)–O(2)	1.943(3)	Zn(1)–O(3)	1.973(3)
Zn(1)–N(3)	2.002(3)	Zn(1)–N(1)	2.017(4)
O(2)–Zn(1)–O(3)	112.44(14)	O(2)–Zn(1)–N(3)	97.18(13)
O(3)–Zn(1)–N(3)	110.32(13)	O(2)–Zn(1)–N(1)	106.51(14)
O(3)–Zn(1)–N(1)	114.49(13)	N(3)–Zn(1)–N(1)	114.57(15)
C(10)–N(3)–Zn(1)	130.3(3)	C(21)–N(1)–Zn(1)	129.3(3)
C(19)–N(1)–Zn(1)	125.4(3)		
Symmetry transformations used to generate equivalent atoms: #1: –x+2, –y+2, –z+1			
Complex **3**			
Mn(1)–O(8)	2.108(3)	Mn(1)–O(1)	2.157(3)
Mn(1)–O(9)	2.227(3)	Mn(1)–N(6)	2.248(3)
Mn(1)–N(8)	2.251(3)	Mn(1)–O(2)	2.394(3)
C(16)$^{\#2}$–O(8)–Mn(1)	149.1(3)	C(16)–O(1)–Mn(1)	118.3(2)
O(8)–Mn(1)–O(1)	117.85(11)	O(8)–Mn(1)–O(9)	147.32(11)
O(1)–Mn(1)–O(9)	94.38(11)	O(8)–Mn(1)–N(6)	86.60(12)
O(1)–Mn(1)–N(6)	84.86(11)	O(9)–Mn(1)–N(6)	91.33(12)
O(8)–Mn(1)–N(8)	90.01(12)	O(1)–Mn(1)–N(8)	96.52(11)
O(9)–Mn(1)–N(8)	91.67(12)	N(6)–Mn(1)–N(8)	176.60(12)
O(8)–Mn(1)–O(2)	90.91(11)	O(1)–Mn(1)–O(2)	150.77(11)
O(9)–Mn(1)–O(2)	56.55(10)	N(6)–Mn(1)–O(2)	92.22(11)
N(8)–Mn(1)–O(2)	88.08(11)	C(19)–O(9)–Mn(1)	94.1(2)
C(19)–O(2)–Mn(1)	86.7(2)	C(5)–N(6)–Mn(1)	129.4(2)
C(10)–N(6)–Mn(1)	124.5(3)	C(21)–N(8)–Mn(1)	126.9(3)
C(22)–N(8)–Mn(1)	128.3(3)		

Symmetry transformations used to generate equivalent atoms:

#1: x+1, y, z+1; #2: –x+1, –y+2, –z+1; #3: x–1, y, z–1

Table 3. Hydrogen Bonds for Complexes 1～3

D–H···A	ARU	d(H···A) (Å)	d(D···A) (Å)	∠(D–H···A) (°)
Complex **1**				
C(2)–H(2)···O(4)		2.57	3.270	133
C(16)–H(16)···O(4)	2–*x*, 2–*y*, –*z*	2.52	3.295	141
C(3)–H(3)···O(4)	1–*x*, 1–*y*, –*z*	2.35	3.191	149
C(37)–H(37)···N(4)	3–*x*, 2–*y*, –*z*	2.53	3.456	175
Complex **2**				
C(7)–H(7)···O(2)		2.43	2.751	100
C(16)–H(16)···N(2)		2.61	2.921	100
C(8)–H(8)···O(3)	2–*x*, 1–*y*, 1–*z*	2.53	3.322	141
C(9)–H(9)···O(4)	3–*x*, 1–*y*, 1–*z*	2.45	3.362	165
C(21)–H(21)···O(4)		2.54	3.123	121
Complex **3**				
C(24)–H(24)···Br(1)	–*x*, 3–*y*, 1–*z*	2.70	3.511	146
C(21)–H(21)···O(1)	–*x*, 2–*y*, 1–*z*	2.42	3.243	147
C(17)–H(17)···O(4)		2.46	2.994	117
C(10)–H(10)···O(2)	1–*x*, 2–*y*, 1–*z*	2.56	3.351	143

Syntheses, Crystal Structures, and Fluorescence Properties of Three Coordination Polymers Constructed Based on Benzoic Acid and Its Derivatives

LIU Guang-Zeng(刘光增)　CHEN Hong-Tai(陈洪太)　ZHANG Xiu-Tang(张修堂)

Three different dimensions CPs have been constructed from the mixed ligands of benzoic acid and its derivatives and two bis(imidazole) linkers (4,4′-bib, 1,4-bmb). The three structures reveal that benzoic acid and its derivatives are effective ligands with rich coordination modes, which is useful to better understand the synthon selectivity in multifunctional crystal structures.